

Fabrication and inter-channel crosstalk analysis of polymer optical waveguides with W-shaped index profile for high-density optical interconnections

Hsiang-Han Hsu,^{1,*} Yusuke Hirobe,¹ and Takaaki Ishigure^{1,2}

¹Graduate School of Science and Technology, Keio University,
3-14-1 Hiyoshi, Kohoku-ku, Yokohama, 223-8522, Japan

²ishigure@appi.keio.ac.jp

*hhhsu@z6.keio.jp

Abstract: For applications in high-density and high-speed optical interconnections, we propose to utilize polymer parallel optical waveguides (PPOWs) with so-called W-shaped refractive index profile in the core area. A W-shaped index profile is composed of a parabolic index distribution surrounded by a narrow index valley, followed by a cladding with a uniform refractive index. We expect that W-shaped index profiles contribute to decreasing the inter-channel crosstalk due to mode conversion in the waveguides. In this paper, we investigate how much the index difference of the index valley improves the crosstalk value. First, we fabricate polymer waveguides with various index profiles by changing the composition of the copolymer for cladding. We show the results that a 1-m long W-shaped profile PPOW has not only low propagation loss (0.027 dB/cm), but an inter-channel crosstalk (~-40 dB) lower than those of graded index (GI) core PPOW we previously fabricated. Next, we theoretically analyze the propagation loss and inter-channel crosstalk in polymer waveguides with different index profiles by means of a ray tracing model in which the light scattering effect is included. The calculation results indicate that the index valley surrounding each core works properly for preventing the power coupling from the cladding modes to the propagation modes, and consequently, very low inter-channel crosstalk is realized with W-shaped index profiles.

©2011 Optical Society of America

OCIS codes: (250.5460) Polymer waveguides; (200.4650) Optical interconnects; (080.5692) Ray trajectories in inhomogeneous media.

References and links

1. A. F. Benner, M. Ignatowski, J. A. Kash, D. M. Kuchta, and M. B. Ritter, "Exploitation of optical interconnects in future server architectures," *IBM J. Res. Develop.* **49**(4), 755–775 (2005), <http://ieeexplore.ieee.org/stamp/stamp.jsp?tp=&arnumber=5388810>.
2. N. Bamiedakis, J. Beals IV, R. V. Penty, I. H. White, J. V. DeGroot, Jr., and T. V. Clapp, "Cost-effective multimode polymer waveguides for high-speed on-board optical interconnects", *IEEE J. Quant. Electron.*, **45**, 415 (2009), <http://ieeexplore.ieee.org/stamp/stamp.jsp?tp=&arnumber=4803864>.
3. I. Papakonstantinou, D. R. Selviah, R. C. A. Pitwon, and D. Milward, "Low-cost, precision, self-alignment technique for coupling laser and photodiode arrays to polymer waveguide arrays on multilayer PCBs", *IEEE Trans. Advanced Packaging*, **31**, 502, (2008), http://ieeexplore.ieee.org/xpls/abs_all.jsp?arnumber=4534823.
4. T. Ishigure and Y. Takeyoshi, "Polymer waveguide with 4-channel graded-index circular cores for parallel optical interconnects," *Opt. Express* **15**(9), 5843–5850 (2007), <http://www.opticsinfobase.org/abstract.cfm?uri=oe-15-9-5843>.
5. Y. Takeyoshi and T. Ishigure, "High-density 2 X 4 channel polymer optical waveguide with graded-index circular cores," *J. Lightwave Technol.* **27**(14), 2852–2861 (2009), <http://www.opticsinfobase.org/abstract.cfm?uri=jlt-27-14-2852>.

6. T. Ishigure and Y. Nitta, "Polymer optical waveguide with multiple graded-index cores for on-board interconnects fabricated using soft-lithography," *Opt. Express* **18**(13), 14191–14201 (2010), <http://www.opticsinfobase.org/oe/abstract.cfm?uri=oe-18-13-14191>.
7. K. Okamoto and T. Okoshi, "Analysis of wave propagation in optical fibers having core with a-power refractive-index distribution and uniform cladding," *IEEE Trans. Microw. Theory Tech.* **24**(7), 416–421 (1976), http://ieeexplore.ieee.org/xpl/freeabs_all.jsp?arnumber=1128869.
8. K. Okamoto and T. Okoshi, "Computer-Aided Synthesis of the Optimum Refractive-Index Profile for a Multimode Fiber," *IEEE Trans. Microw. Theory Tech.* **25**(3), 213–221 (1977), http://ieeexplore.ieee.org/xpl/freeabs_all.jsp?arnumber=1129073.
9. K. Oyamada and T. Okoshi, "High-accuracy numerical data of propagation characteristics of a-power graded-core fibers," *IEEE Trans. Microw. Theory Tech.* **28**(10), 1113–1118 (1980), http://ieeexplore.ieee.org/xpl/freeabs_all.jsp?arnumber=1130234.
10. D. Donlagi'c, "Opportunities to enhance multimode fiber links by application of overfilled launch," *J. Lightwave Technol.* **23**, 35264 (2005), <http://www.opticsinfobase.org/abstract.cfm?uri=JLT-23-11-3526>.
11. T. Ishigure, H. Endo, K. Ohdoko, K. Takahashi, and Y. Koike, "Modal bandwidth enhancement in a plastic optical fiber by W-refractive index profile," *J. Lightwave Technol.* **23**(4), 1754–1762 (2005), <http://www.opticsinfobase.org/abstract.cfm?uri=JLT-23-4-1754>.
12. K. Takahashi, T. Ishigure, and Y. Koike, "Index profile design for high-bandwidth W-shaped plastic optical fiber," *J. Lightwave Technol.* **24**(7), 2867–2876 (2006), <http://www.opticsinfobase.org/abstract.cfm?uri=JLT-24-7-2867>.
13. Y. Takeyoshi and T. Ishigure, "Multichannel parallel polymer waveguide with circular W-shaped index profile cores," *IEEE Photon. Technol. Lett.* **19**(22), 1795–1797 (2007), <http://ieeexplore.ieee.org/iel5/68/4351987/04367530.pdf?arnumber=4367530>.
14. H. H. Hsu and T. Ishigure, "High-density channel alignment of graded index core polymer optical waveguide and its crosstalk analysis with ray tracing method," *Opt. Express* **18**(13), 13368–13378 (2010), <http://www.opticsinfobase.org/abstract.cfm?uri=oe-18-13-13368>.
15. H. M. Presby, W. Mammel, and R. M. Derosier, "Refractive index profiling of graded index optical fibers", *Rev. Sci. Instrum.*, **47**, 348 (1976), http://ieeexplore.ieee.org/xpl/freeabs_all.jsp?tp=&arnumber=4981006.
16. A. W. Snyder and J. D. Love, *Optical Waveguide Theory* (Chapman & Hall, 1983), Chap. 7, <http://goo.gl/k3Z9m>.

1. Introduction

The increasing requirement of calculation power provided by high performance computers (HPCs) leads a trend in board level data communication from electrical to optical interconnection [1]. Hence, several kinds of optical waveguides have been developed for the purpose of high data rate, low power dissipation, high bandwidth-distance product, and low propagation loss. In particular, multimode and multi-channel polymer optical waveguides have been presented to be high performance data communication devices. The advantages of multimode waveguides are in their large core size (several tens of micrometers in width and height) compared to the single mode counterparts, because of which the integration scheme of the waveguides on printed circuit boards (PCBs) becomes much simpler. Therefore, a wide variety of polymer materials have been explored for realizing multimode waveguides for on-board applications, and in general, most of the polymer waveguides have been prepared by photolithography or imprinting techniques. Furthermore, the demand for much higher-density parallel data transmission even on PCBs leads to a dense alignment of the channels even for optical waveguides. However, in such an optical waveguide with extra-narrow inter-core pitch, the inter-channel crosstalk could become no longer ignorable. Actually, inter-channel crosstalk in polymer multimode waveguides is already discussed in some reports [2,3].

To address this crosstalk problem, several methods have been proposed, and we have been investigating polymer parallel optical waveguides (PPOWs) with graded-index (GI) cores [4-6]. Then, we confirmed that the quadratic index profile confined the optical field near the core center, consequently, the crosstalk dramatically decreased even under very narrow pitch. Furthermore, we have focused on the *mode conversion* from cladding modes to propagation modes, which dominates the origin of inter-channel crosstalk in current polymer waveguides with a pitch as wide as 250 μm . In this paper, we focus on so called W-shaped refractive index profile for further crosstalk reduction, and how the profile influences the optical performance.

W-shaped index profiles were discussed for minimizing the modal dispersion with axial symmetric core media more than twenty years ago and the optimum refractive index profile for multimode fibers was designed. Here, a W-shaped index profile is composed of a parabolic index distribution surrounded by a narrow *index valley*, followed by a cladding with a uniform refractive index. The improvement of modal dispersion by W-shaped index profiles was reported by Okamoto et al. [7-9], and similar trials were also reported in [10]. Furthermore, the ability to minimize the modal dispersion with a W-shaped index profile is also confirmed experimentally and theoretically in polymer optical fibers (POFs) [11, 12]. In [12], we adjust the concentration of benzyl methacrylate (BzMA) in the copolymer for the cladding to obtain a different depth of the index valley. Furthermore, in our previous study, we preliminarily verified a crosstalk reduction due to a W-shaped refractive index profile [13] with only a shallow index valley.

In this paper, we adopt the fabrication method reported in [12] to adjust the index valley, and then follow the similar technique reported in [13] to fabricate several multi-channel PPOWs with W-shaped index profile (W-shaped PPOWs). Meanwhile, for a theoretical analysis of propagation loss and crosstalk in W-shaped PPOWs, we apply the previously developed ray tracing method that involves the light scattering effect [14]. We show not only some experimental results on the inter-channel crosstalk with respect to several different depth of index valley, but also theoretically simulate the near field patterns (NFPs) from the output ends in order to verify the inter-channel crosstalk advantage of these featured waveguides.

2. Waveguide fabrication and characterization

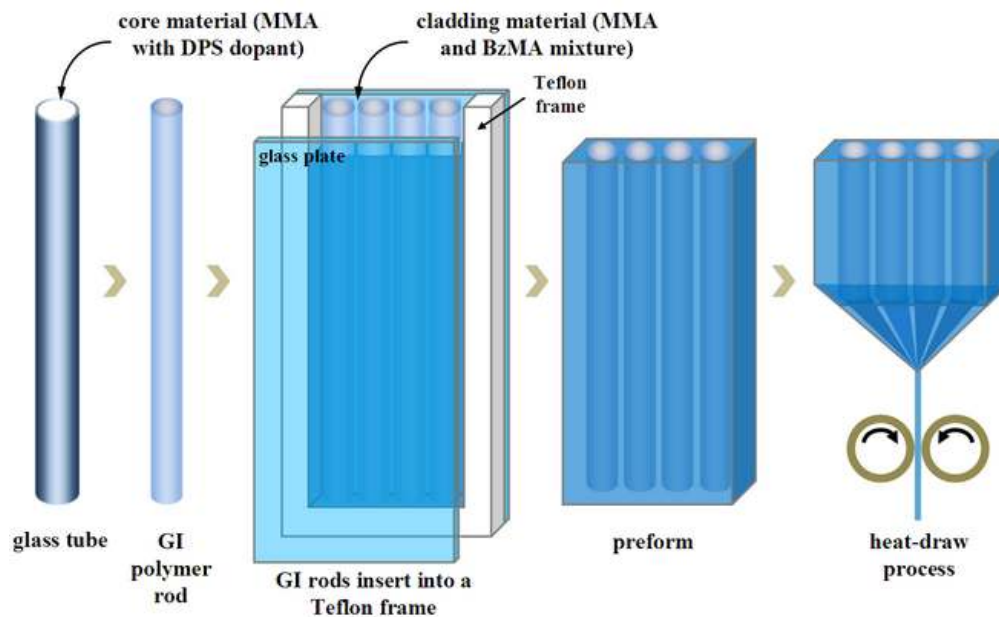


Fig. 1. Fabrication process of W-shaped refractive index profile PPOW.

The fabrication process of W-shaped PPOWs employed in this paper is shown in Fig. 1. It is based on the preform method in which the refractive index of cladding is controlled by adjusting the feed concentration of BzMA monomer to methyl methacrylate (MMA) monomer [12]. Here, a graded refractive index distribution modeled by the power-law form shown by Eq. (1) should be formed in each circular core (channel) area. Outside each core area, a refractive index valley is added, and the refractive index profile $n(r)$ as a function of the distance r from the core center is written with a parameter of index exponent g as,

$$\begin{cases} n(r) = n_1[1 - 2\Delta(r/a)^8]^{1/2}, & 0 \leq r \leq a \\ n(r) = n_2, & a < r \leq (a+w) \\ n(r) = n_3, & (a+w) < r \end{cases} \quad (1)$$

where, Δ is the relative refractive index difference, a is the core radius, and w is the width of the valley. In addition, n_1 is the highest refractive index value in the core region (normally at the core center), n_2 is the lowest refractive index of the valley, and n_3 is the refractive index of the cladding which is larger than n_2 . If n_2 and n_3 are equal, a GI refractive index profile is described by the same equation.

The first step is to fabricate several GI rods for the cores of the W-shaped waveguides, as shown in Fig. 1. Several 50-cm long glass tubes with 10-mm inner diameter are filled with a specified amount of MMA monomer with a polymerization initiator and chain transfer agent. The tube is rotated on its axis at 2000 to 3000 rpm in an oven at 70 °C. After several hours of polymerization reaction, a hollow PMMA tube is formed. Then, we remove the glass tube and fill the PMMA tubes with the core material, and heat up the tubes in an oil bath at 120 °C in order to polymerize the core material. Here, the core material is composed of MMA monomer doped with an 11 wt. % of diphenyl sulfide (DPS). After the polymerization completes, a rod with a near-parabolic refractive index profile is obtained. This method, named the interfacial-gel polymerization technique, is already well established as a preparation method of GI polymer optical fiber [11].

Next, we arrange those GI rods in a line and insert them in a mold composed of a Teflon frame and two glass plates, as shown in Fig. 1. Then, the space between the inner mold and GI rods are filled with a plenty of MMA and BzMA monomer mixture, followed by polymerization of the monomer to form a preform plate. In the obtained preform plate, the GI core in all the rods are surrounded by a thin PMMA-homopolymer layer, while the outermost layer is composed of a PMMA-BzMA copolymer. Since the refractive index of BzMA is higher than that of PMMA, the PMMA homopolymer layer works as a refractive index valley in a W-shaped index profile. After heat-drawing the preform, a multi-channel W-shaped PPOW is obtained

2.1 Near field pattern and propagation loss

Figure 2 shows the cross-section of W-shaped and GI waveguides illuminated by a Halogen-Tungsten lamp at the input ends. Note that in the case of W-shaped waveguide, as Fig. 2(a) shows, even if the waveguide is launched under the overfilled mode launching (OML) condition, a dark ring is observed around each core, which corresponds to the refractive index valley. This implies most of the light may either couple to one of the cores or be restrained inside the cladding, and hardly remain at the index valley. This phenomenon will be simulated and discussed in later pages.



Fig. 2. (a) W-shaped and (b) previously obtained GI-PPOW illuminated by a Halogen-Tungsten lamp.

As mentioned in the previous section, we applied the same composition of the core material for both waveguides. So, the optical performance of the GI and W-shaped PPOWs such as numerical aperture (NA), propagation loss, etc., is expected to be similar. Here, we evaluate the effect of the index valley in the W-shaped waveguide by observing the output near field pattern (NFP) under a restricted mode launch (RML) condition that uses a single-

mode fiber (SMF) probe. Figure 3(a) and (c) show the results of GI and W-shaped PPOW, respectively, when the SMF probe is butt-coupled to the center of the far-left edge core, while Fig. 3(b) and (d) are launched at the over-cladding area between the far-left edge and second cores. As we expected, similar NFPs are shown in Fig. 3(a) and (c), by which we confirm similar optical field confinement near the core center. However, when the cladding modes are selectively launched, as in Fig. 3(b) and (d), the W-shaped refractive index profile is apparently advantageous for preventing the cladding light from re-coupling to the adjacent cores. We show this light localization in the cladding improves the inter-channel crosstalk due to mode conversion from the cladding modes to propagating modes in cores [14].

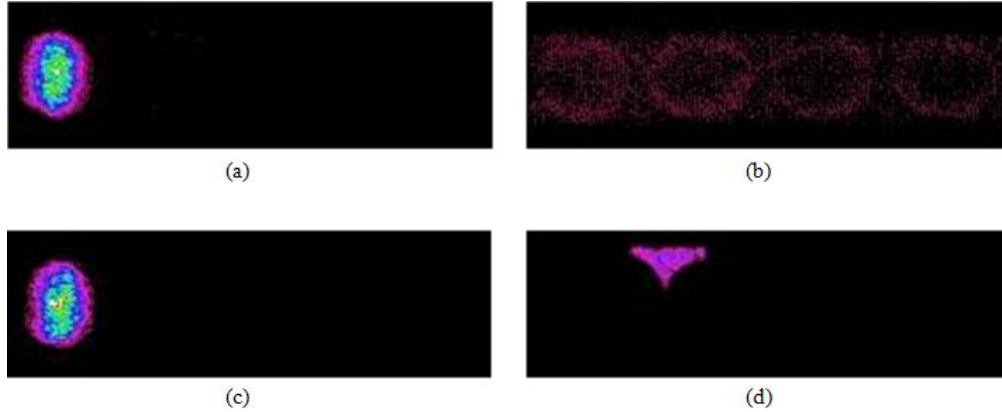


Fig. 3. Near-field patterns of GI PPOW (a) when the core center and (b) cladding are launched and W-shaped PPOW (c) when the core center and (d) cladding are launched.

On the other hand, the propagation loss of the obtained W-shaped waveguide is evaluated by utilizing the cut-back method [12]. In this measurement, incoherent light from a Halogen-Tungsten lamp is coupled to a core of the waveguide via a 50- μm core multimode fiber (MMF) probe (1-m long), and the output light from the core is coupled to another 50- μm core MMF probe to guide to an optical spectrum analyzer (ANDO AQ-6315B). From the slope of the output power variation at a wavelength of 850 nm as shown in Fig. 4 (red points), the propagation loss is obtained as 0.027 dB/cm, which is very close to that (0.028 dB/cm) of the previously obtained GI-PPOW (blue points) [4,5]. In Fig. 4 we also indicate an averaged loss (0.01 dB/cm) of a typical step index (SI) type waveguide for a comparison. We confirm that the newly developed W-shaped PPOW maintains the features of both good optical field confinement and low propagation loss.

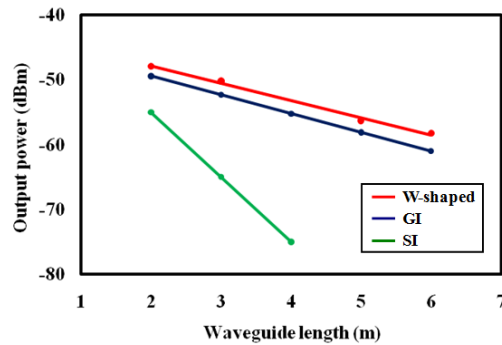


Fig. 4. Propagation loss of SI, GI, and W-shaped PPOW.

2.2 Refractive index profile and inter-channel crosstalk

Referring to the NFP shown in Fig. 3(d), the W-shaped refractive index profile reduces the re-coupling of cladding modes to propagating modes in the adjacent cores. This implies the inter-channel crosstalk also can be reduced. How the light can be restrained in the cladding depends on the depth of the refractive index valley, namely, the index profile. The interference fringe images measured for slab samples of the two waveguides are shown in Fig. 5 (top), and their refractive index profiles are calculated from the fringe patterns, as shown in Fig. 5 (bottom). Here, the waveguide samples for the measurement are fabricated to have a thickness of approximately 200 μm , and then an interference fringe image observed by a dual beam interference microscope with Mach-Zehnder geometry is obtained as Fig. 5 (top) [15]. These results indicate that the similar quadratic index distribution is formed inside the both cores, while an explicit difference is observed in the vicinity of core-cladding boundary, where an index valley exists in the W-shaped PPOW as shown in Fig. 5(a). In order to clarify how much the depth of the index valley really contributes to the inter-channel crosstalk reduction, we adjust the concentration of BzMA in MMA monomer from 3.66 to 25 wt. % for the cladding, by which the refractive index of outermost cladding is varied as summarized in Table 1. Here, as the refractive index of the bottom of index valley is almost uniform (1.492), the depth of the index valley is varied. Note that when the concentration of BzMA is higher than 15 wt. %, the refractive index of cladding is even higher than that of the core center.

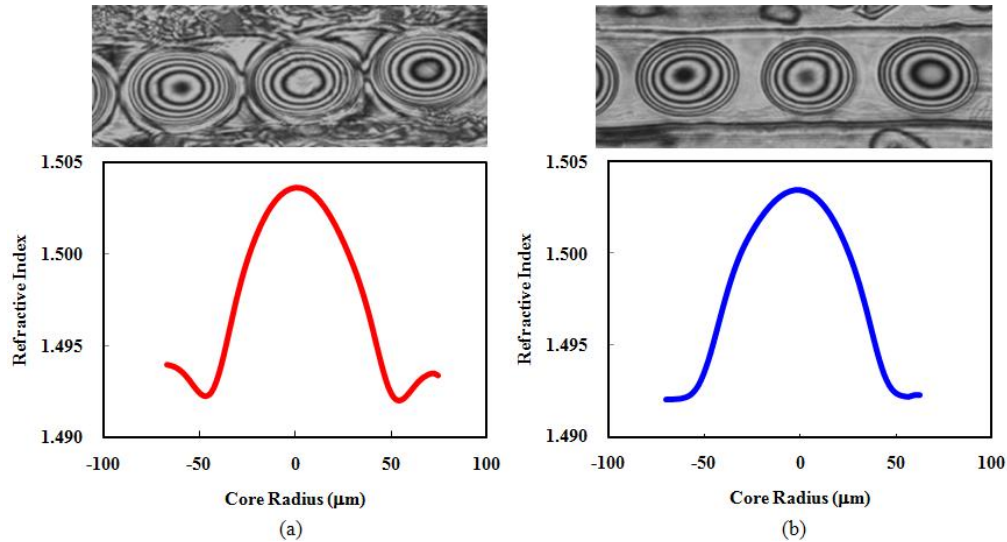


Fig. 5. The interference fringe patterns (top) and its corresponding refractive index profile (bottom) of (a) GI (b) W-shaped profile with 3.66 wt. % BzMA PPOW.



Fig. 6. Experiment setup for inter-channel crosstalk measurement.

The definition of the inter-channel crosstalk (XT) is expressed as the following equation:

$$XT(dB) = 10 \log \frac{I_1}{I_0} \quad (2)$$

where, I_0 is the output intensity from the launched core and I_1 is from one of the adjacent cores. We characterize the inter-channel crosstalk using the experimental setup shown in Fig. 6. The waveguides in this measurement are 1-m in length. One of the cores is launched via an SMF probe or an MMF probe with a 50- μm core diameter, which corresponds to RML and near OML conditions, respectively. The output power from the specified points on the cross-section of the output end was measured using another MMF probe for detection.

Figure 7 shows the comparison of GI core and W-shaped profile with 10 wt. % of BzMA in the outermost cladding. In the case of W-shaped PPOW under the RML condition as shown in Fig. 7(a), the other three cores show almost no detectable output intensity. Meanwhile, in Fig. 7(b), under the near OML condition, an output power of -55 dBm is observed both from the cladding and other cores in the W-shaped PPOW. However, the output intensity from the right edge core is even weaker than that of the cladding. Under both launching conditions, the output power from the GI waveguide (blue curve) is higher than that from the W-shaped waveguide (red curve). We confirm that the W-shaped profile effectively reduce the crosstalk. Table 1 shows the numerical results of different waveguides under both RML and near OML conditions. The crosstalk values in Table 1 are measured at the center of the right-neighbor core. Note that under the near OML condition, when the concentration of BzMA is 10 wt.%, the crosstalk value as low as -40.3 dB is observed, while the crosstalk value instead increases with increasing the concentration of BzMA in the cladding from 10 wt. % to 20 wt. %. As we already confirmed in Fig. 3, the lower crosstalk in W-shaped PPOW than in GI one is attributed to low mode conversion from cladding modes to propagating modes. However, when the BzMA concentration is higher than 20 wt. %, the refractive index of the outermost layer is higher than that of the core center, and thus, the light could be well confined in the outermost layer. Therefore, the crosstalk decreases again to the minimum at 25 wt. % of BzMA concentration. In the case when BzMA concentration is 10 wt.%, n_3 is 1.499 which is almost half value between the core center (1.504) and the bottom of valley (1.492), which could be optimum.

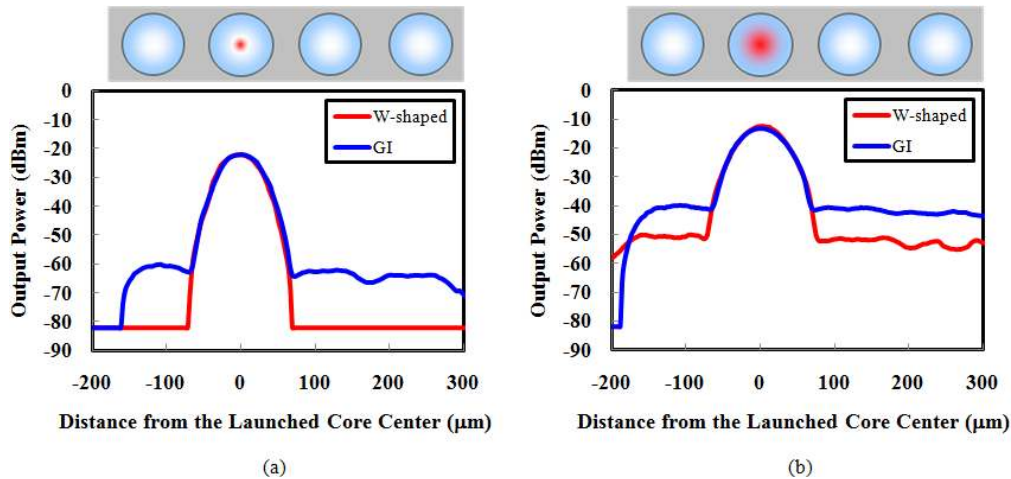


Fig. 7. Output intensity when one of the cores (second from the left) in waveguides is launched via (a) SMF probe (RML condition) and (b) MMF probe (near OML condition). The concentration of BzMA for W-shaped profile PPOW here is 10 wt. %.

Table 1. Relationship Between Crosstalk Value and Refractive Index of the Cladding With Corresponding Concentration of BzMA

Waveguide type	Refractive Index of the cladding	Crosstalk value (RML condition)	Crosstalk value (near OML condition)
GI	1.492	-40.1 dB	-27.5 dB
W-shaped (3.66 wt. %)	1.495	< -59.6 dB	-32.0 dB
W-shaped (10 wt. %)	1.499	< -59.8 dB	-40.3 dB
W-shaped (15 wt. %)	1.502	< -59.6 dB	-36.1 dB
W-shaped (20 wt. %)	1.506	< -44.3 dB	-33.5 dB
W-shaped (25 wt. %)	1.509	< -59.2 dB	-41.5 dB

2.3 Inter-channel crosstalk in short length waveguides

For board level optical interconnections, the physical dimension of the optical waveguides generally could be centimeter scale in length. In this part, we apply 5-cm long waveguides with both index profiles to the same experimental setup as shown in Fig. 6. Table 2 shows the results of these short waveguides. Compared to the results in Table 1, the crosstalk reduction by a W-shaped profile is not apparent in the shorter waveguide. Actually, only about a 6-dB difference in crosstalk value is observed between the W-shaped and GI PPOWs in Table 2 (MMF launch), while there is a 12.8-dB difference between the corresponding waveguides in Table 1.

Table 2. Crosstalk Value in 5-cm GI and W-Shaped PPOWs

Waveguide type	Crosstalk value (launched by SMF)	Crosstalk value (launched by MMF)
GI	< -61.1 dB	-33.7 dB
W-shaped (10 wt. %)	< -61.3 dB	-39.6 dB

3. Theoretical analysis of inter-channel crosstalk for W-Shaped PPOW

We already developed a ray tracing simulation program to analyze the propagation loss and inter-channel crosstalk in PPOWs taking the light scattering effect into consideration [14]. From the ray optics point of view, when a ray in the cladding propagates toward the boundary of valley and cladding, either it reflects back or penetrates into the index valley, depending on the incident angle. Here, our concern is how the rays behave in the vicinity of steep and gradually varying index valleys. In Fig. 8(a), one of the measured refractive index profiles $n(r)$ corresponding to a BzMA concentration of 10 wt. % is drawn with the yellow (round dotted) curve. Actually, a gradually-varying index valley (not a steep one) is observed. The gradual index variation is actually observed at the interface between the index valley and cladding shown in Fig. 8(a) in our waveguide samples. This index variation is formed with the same mechanism as that of the parabolic index profile in the core region. The outermost layer of GI rods composed of PMMA homopolymer is slightly swollen to the monomer mixture of MMA and BzMA, when the rods are inserted in the Teflon frame, as shown in Fig. 1. Then, a gradual concentration distribution of MMA-BzMA is formed around the boundary, which makes the gradual index change at the interface between the index valley (PMMA layer) and cladding.

The calculated ray-trajectories with incident angles from 84.7° to 84.9° are shown in the right side of Fig. 8(a). Here, the incident rays are injected from the outside of the index valley (at $r = 90 \mu\text{m}$). It is clearly illustrated that the rays with an incident angle lower than 84.5° penetrate into the core, while the rays with an incident angle higher than 84.5° follow the trajectory similar to the “reflected” rays. The angle of 84.5° is very close to the theoretically calculated critical angle ($\sin^{-1}(1.492/1.499) = 84.461^\circ$). Hence, in the developed ray tracing simulation, we confirm that the trajectory of light in such a narrow area like 10- μm thick index valley is calculated properly. This gives us a reasonable approximation for applying Eq. (1) to theoretical model. The modeled refractive index profile is shown in Fig. 8(b), where a steep index valley is applied.

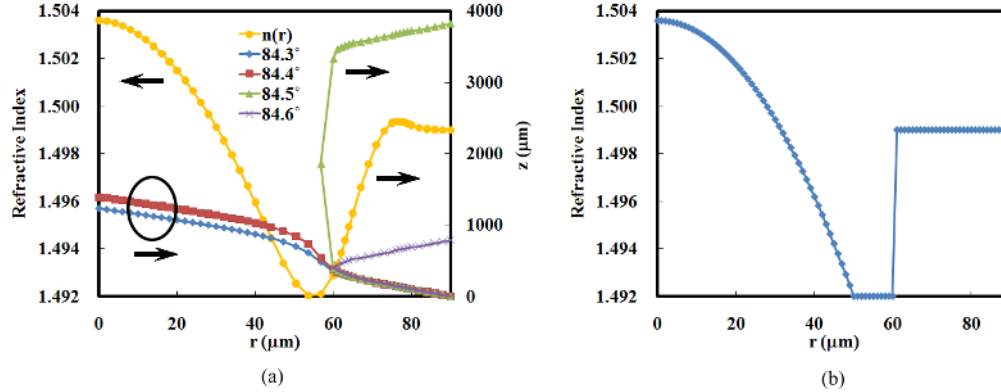


Fig. 8. (a) The measured refractive index profile of W-shaped profile PPOW with 10 wt. % BzMA in cladding. In the right side are the calculated ray trajectories with different incident angles. (b) The theoretical modeling of refractive index profile according to Eq. (1).

The parameters for the calculation are listed in Table 3. The core radius is $50 \mu\text{m}$, where the refractive index of the core center is 1.5036, refractive index of the bottom of valley is 1.492, and the core pitch is $100 \mu\text{m}$, all of which are identical to those of the fabricated waveguide. The index exponent g is set to 2.0 as the parabolic index profile within the core area. Furthermore, in order to include the light scattering effect in ray tracing, three parameters are incorporated: probability of scattering (p), maximum number of split rays after one scattering (N_s) and maximum angle difference of scattered ray to the original ray direction (θ_m) [14]. The parameter p is set to a predetermined value from 0 to 1 for the calculation. During the ray tracing, we randomly add the “light scattering” event to split the original ray to several (N_s) rays using random numbers also ranging from 0 to 1. The ray splits when the random number is smaller than the predetermined p value at each decision point along with the ray trajectory. Therefore, when the p value is set to 1, the scattering occurs at all the decision points, while no scattering occurs when p is 0. The N_s and θ_m are set to be 2 and 10, respectively. We preliminary confirmed if two same values of scattering loss are observed under different combinations of N_s , θ_m , and p , the crosstalk values under these two settings were almost the same. Therefore, we regard that these settings are good enough. Furthermore, in order to obtain the relationship between the refractive index valley depth and inter-channel crosstalk, four n_3 values (1.492, 1.495, 1.499, and 1.502) are applied. Furthermore, we assume a low-loss and very-lossy core materials, which correspond to the parameter p of 0.02 and 1, respectively. For more promising calculation results and shortening the calculation time, we focus on the performance of short waveguide length (~ 5 cm). After tracing all of the rays (bound, tunneling, reflected, and refracted rays [16]), the intensity and location information of each ray is stored. Then, the propagation loss and crosstalk values are quantitatively calculated at the output end of the waveguide.

Table 3. Parameters for Calculation by Ray Tracing Method

Parameters	Value
Core radius (a)	$50 \mu\text{m}$
Index valley width (w)	$10 \mu\text{m}$
Refractive index of core center (n_1)	1.5036
Refractive index of valley (n_2)	1.492
Index exponent (g)	2
Core pitch	$100 \mu\text{m}$

3.1 Launching condition

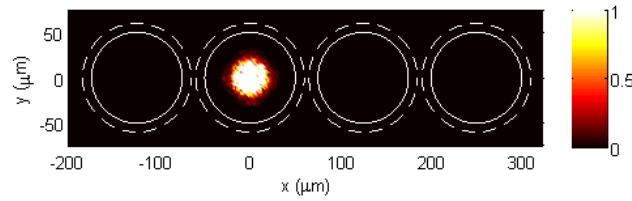


Fig. 9. The launching condition for the simulation. We apply the same condition as the experimental setup in which the second core from the left side is launched by an MMF (50 μm in diameter).

According to the experimental results, we can visually observe some light leakage outside the launched core at the output end in the case under the MMF launch. This implies the inter-channel crosstalk is unavoidable under this launching condition. Here, we pay attention to the difference between GI and W-shaped PPOWs. We assume that there are four cores in the calculation model and that the second core from the left is launched with a spot size of 50 μm at the core center. Under this launching condition, approximately 5000 rays form a 2D Gaussian profile as shown in Fig. 9. The intensity of the left core, right core, and cladding are expressed as I_{left} , I_{right} , and I_{clad} , respectively, which are initially set to zero at the launching plain ($z = 0$). In Fig. 9, the inner white circles indicate the core/valley boundary; the white dotted circles indicate the outer edge of the valley. The medium outside the waveguide is air ($n_{air} = 1$).

3.2 Calculation results for very lossy condition

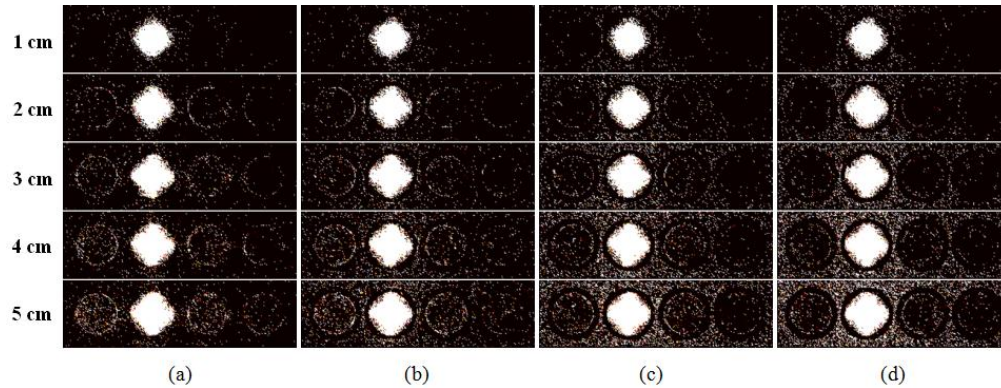


Fig. 10. Calculated NFP and propagation loss with corresponding output end (1 cm to 5 cm) for various refractive index of cladding under very lossy condition: (a) 1.492 (GI), 0.56 dB/cm (b) 1.495 (3.66 wt. % of BzMA), 0.58 dB/cm (c) 1.499 (10 wt. % of BzMA), 0.60 dB/cm (d) 1.502 (15 wt. % of BzMA), 0.60 dB/cm.

First, a very lossy condition ($p = 1$) is considered and the calculated NFPs are shown in Fig. 10. In these calculated NFP data, we remove the white-color boundary shown in Fig. 9, while we adjust the color map to clearly visualize the weak output intensity. In Fig. 10, we observe the length dependence of NFP which shows the light gradually diffuses toward the cladding area. In the case of W-shaped PPOW (Fig. 10(b), (c), and (d)), the index valley around each core is confirmed as a dark ring, which is also observed in the NFP experimentally obtained in Fig. 2(a). Furthermore, compare to the GI PPOW shown in Fig. 10(a), with increasing the depth of index valley, the core areas except for the launched one are visualized more clearly as dark circles. The dark cores indicate low output power (low crosstalk).

Figure 11 shows the numerical results of absolute output intensity and crosstalk values. In Fig. 11(a), the output intensity from the launched cores (I_{mid}), shows that the trend decreases

linearly with respect to the waveguide length in all PPOWs including the GI case ($n_2 = 1.492$), which indicates that the propagation loss due to scattering is almost identical in all the waveguides. From the slope of Fig. 11 (a), the propagation loss (due to scattering) of these waveguides is calculated to be 0.58 - 0.60 dB/cm, which is quite high. On the contrary, the output intensity from the whole cladding, I_{clad} , obviously depends on n_3 value, and in the case of the highest $n_3 = 1.502$, I_{clad} is the highest for any waveguide length. Hence, we can conclude that the larger the difference of n_2 and n_3 , the higher intensity remains in the cladding. Moreover, when there is no index valley ($n_3 = 1.492$), once the light is scattered from the launched core, it may easily re-couple to the other cores and increase the crosstalk value. Actually, as shown in Fig. 11(c) and (d), the crosstalk value (XT) decreases with increasing the depth of index valley (higher n_3 value), and approximately 5 dB difference in crosstalk is observed between the GI and W-shaped PPOW with the deepest valley after a 5-cm propagation.

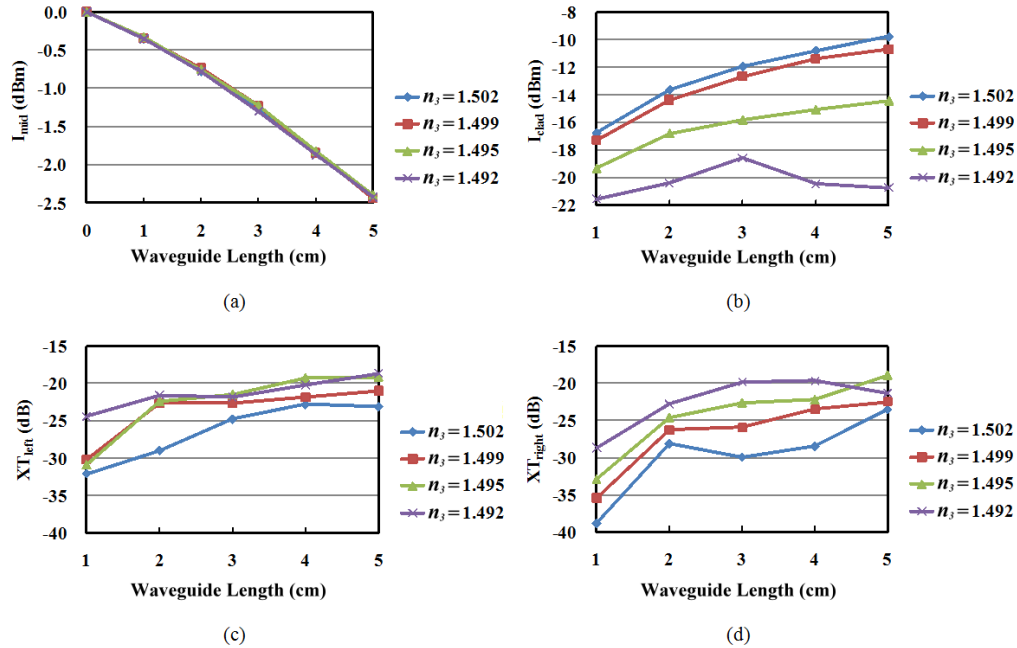


Fig. 11. Calculated results by ray trace simulation: (a) Output intensity from the launched core. (b) Output intensity from the whole cladding. (c) Crosstalk value (XT) to the left-edge core. (d) Crosstalk value to the third core from the left edge.

3.3 Calculation results for low-scattering-loss condition

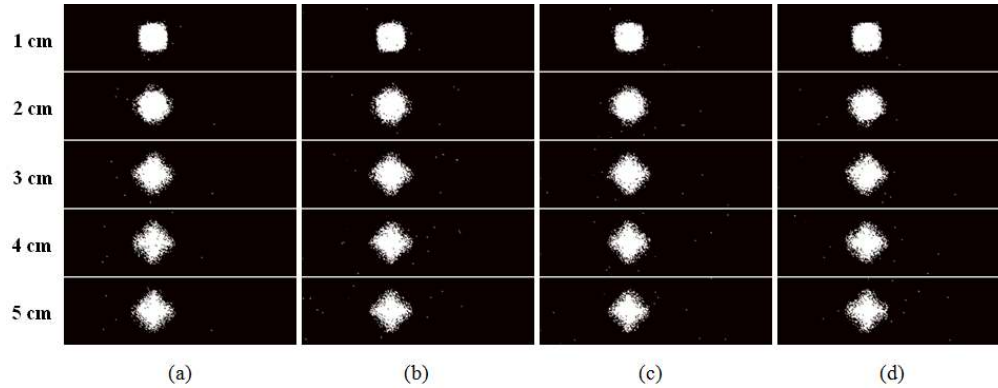


Fig. 12. Calculated NFP and propagation loss of W-shaped PPOWs with various refractive index of cladding compared to that of GI PPOW: (a) 1.492 (GI), 0.26 dB/cm (b) 1.495 (3.66 wt. % of BzMA), 0.26 dB/cm (c) 1.499 (10 wt. % of BzMA), 0.27 dB/cm (d) 1.502 (15 wt. % of BzMA), 0.26 dB/cm.

In order to simulate real applications for board-level optical interconnections, we should consider lower-loss conditions than that in the previous section, because the propagation loss of 0.6 dB/cm calculated in Fig. 10 is too high compared to those of actually obtained waveguides. Therefore, in the calculation of this section, the scattering probability p is set to 0.02. In this case, the propagation loss is calculated to be 0.26 - 0.27 dB/cm. The calculated NFPs and numerical results are shown in Fig. 12 and Fig. 13, respectively. In Fig. 12, all the cases show very similar results that the adjacent cores have very weak output intensities, namely, very low crosstalk. Figure 13(a) shows similar trend to Fig. 11(a); the propagation loss still identical in all the waveguides. We observe the highest output intensity from the cladding when the index valley depth is the highest ($n_3 = 1.502$) as shown in Fig. 13(b). However, it is noteworthy that the absolute value of I_{clad} is much smaller than that in Fig. 11 (b). The crosstalk values are shown in Fig. 13(c) and (d), where some empty values indicate no rays could be counted. Some unexpected fluctuations in the XT value are observed because the optical power coupled to the other cores is too low. Hence, the W-shaped index profile is effective for reducing the inter-channel crosstalk mainly due to mode conversion, particularly when polymer waveguides are composed of polymer materials that exhibit essentially high scattering loss. Therefore, with increasing the waveguide length, the W-shaped index profile works more effectively, as experimentally shown in Tables 1 and 2, since the longer length propagation corresponds to high probability or scattering (highly accumulated scattering loss).

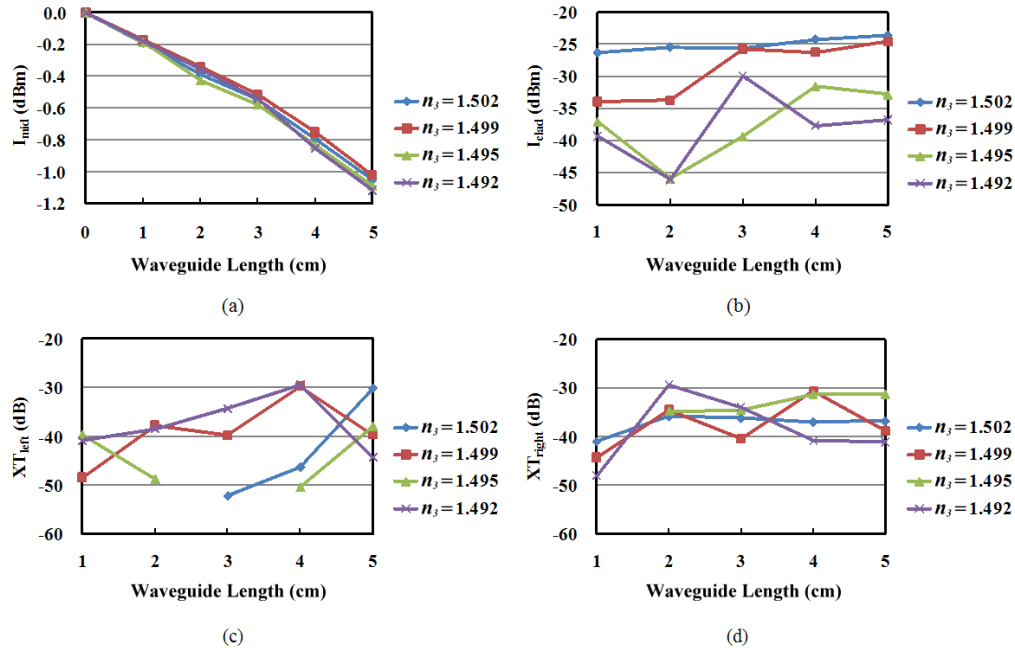


Fig. 13. Calculated results by ray trace simulation (a) Output intensity from the launched core. (b) Output intensity from the whole cladding. (c) Crosstalk value (XT) to the left-edge core. (d) Crosstalk value to the third core from the left edge.

4. Conclusion

We successfully fabricated W-shaped PPOWs with desired refractive index profiles. This is a reliable solution that can simultaneously realize low propagation loss (0.027 dB/cm) and low inter-channel crosstalk (-40.3 dB). In the case of higher concentration of BzMA in the cladding material, it realizes an unexpectedly higher crosstalk value which could result from the higher refractive index of cladding (outermost layer) than that of the cores.

It is theoretically confirmed that the larger the depth of index valley, the lower inter-channel crosstalk. Furthermore, for centimeter scale optical interconnections, we apply the ray tracing method to confirm the advantages of W-shaped profile PPOW visually and numerically. We conclude that W-shaped refractive index profiles perform as low propagation loss as GI waveguides with the additional characteristic of inter-channel crosstalk suppression for the application of high dense aligned optical interconnections.